"On the fly" characterization of Yb^{III}:Er^{III} co-doped upconversion nanoparticle nonlinear optical response from single-particle trajectories

Isabela N. Cavalcante,[a] M. Claudia Marchi,[b,c] Fernando A. Sigoli,[a] Paulo C. de Sousa Filho,[a] Beatriz C. Barja,*[b,c] and René A. Nome*[a]

[a] Institute of Chemistry, University of Campinas, Brazil, 13083-970.

E-mail: nome@unicamp.br

[b] University of Buenos Aires, Buenos Aires, Argentina

E-mail: barja@qi.fcen.uba.ar

[c] INQUIMAE, CONICET, Argentina

Abstract: Spectroscopic characterization of individual nanoparticles is essential for understanding their structure-property relationship and for applications. Upconversion nanoparticles (UCNPs) in condensed phases can undergo both nonlinear optical and stochastic dynamics when interacting with near-infrared sources. By integrating optical trapping micro-spectroscopy, stochastic dynamics and light-matter interactions experiments and simulations, in the present work we study how individual trajectories of Yb^{III}:Er^{III} co-doped UCNPs can be used to perform "on the fly" characterization of their nonlinear optical power-law response upon near-infrared excitation. We illustrate the methodology in the case of freely diffusing and optically trapped UCNPs as well as with particles bound to the substrate. The approach presented in this work can be applied to UCNPs with varying composition and morphological features, particularly in single-particle studies.

Introduction

What can we learn by integrating dynamical information occurring at different timescales? Fundamental timescales associated with atomic motion are orders of magnitude shorter than processes occurring in real time, such as catalysis, nucleation and crystal growth, macromolecular self-assembly, and molecular biological processes, among others.[1-4] In many cases, a two-state energy landscape separated by a barrier captures essential features of the dynamics and kinetics in thermally activated processes. Therefore, a stochastic approach can be used whereby the system's dynamics is described as diffusion at the bottom of the reactant well and diffusive crossing across the transition state barrier. As a result, to characterize the full dynamics of the problem, one needs to characterize both the barrier crossing time and the reactant well residence time. These two diffusive processes can occur in vastly different timescales, and yet both are needed to describe the full dynamics. Although this general picture is useful to show why should one care about timescale integration in chemistry, it is interesting to consider this connection in other settings as well, not necessarily involving barrier crossing. Additionally, it is important to apply these ideas to specific chemical systems exhibiting response at distinct timescales. Within this context, in the present work we sought to apply the timescale integration perspective to describe the stochastic dynamics and nonlinear optical response of upconversion nanoparticles.

Upconversion nanoparticles (UCNPs) combine the special spectroscopic properties of rare-earth-based materials with the generation of sensitive and controllable optical responses at the nanoscale, which make them extremely attractive tools for applications in biology, industry, environment, and security.[5-8] UCNPs are interesting systems for studying the connection

between Brownian motion and time-resolved nonlinear optical spectroscopy because multiple timescales are required to describe the UCNP stochastic dynamics and photophysics, from the earliest events following light absorption on the femtosecond timescale up to microseconds, which are typical radiative lifetimes for UCNPs.[9-11]

Upconversion luminescence in UCNPs is characterized by a complex interplay of competing nonlinear optical responses occurring at any order, including for example, excited state absorption and cooperative as well as sequential energy transfer, among others.[12-15] Detailed studies of light-matter interaction mechanisms and the resulting upconversion power dependence are essential in basic research and for the improvement of device performance.[10,13] In the case of a macroscopic sample containing an ensemble of UCNPs, this nonlinear optical spectroscopic characterization involves the measurement of UCNP emission intensity and spectra as a function of incident intensity. A double-logarithmic plot of incident and emitted intensities then gives the linearized power dependence, which is the power law describing the material nonlinear optical response in the incident intensity range studied.

In addition to ensemble measurements, assessing the nonlinear optical response at the single-particle level enables further studies relating structure to property, since UCNP nanoparticle composition and morphology influence upconversion emission intensities. Recently, single UCNP power dependence studies performed by optical trapping measurements have been reported [16], which enabled characterization of the nonlinear optical properties of individual nanoparticles and comparison with ensemble measurements. In the work described in reference [16], the authors varied the intensity of the trapping laser beam while monitoring UCNP emission to record their power dependence.

Previously, we have reported the stochastic dynamics study of co-doped Yb^{III}:Er^{III} UCNPs.[17] HR-SEM images revealed these UCNPs exhibited average diameter of 400 nm. We have used a nonlinear micro-spectroscopy setup to excite the UCNPs at 980 nm and recorded images and spectra in the visible spectral range. Additionally, we have employed quantitative optical microscopy analysis to register UCNP emission intensity and particle position as a function of time. The stochastic trajectories of individual UCNPs were characterized by a combination of Brownian motion, particle-substrate interactions and optical forces. We have used a stochastic dynamics model including viscoelasticity, rotational diffusion, and optical forces to describe the experimentally retrieved individual nanoparticle trajectories as well as the time-dependent mean-squared displacement.

On the other hand, we have also studied the photophysics of hierarchically structured core / triple-shell, co-doped Nd^{III}:Yb^{III}:Er^{III} UCNPs excited by CW and femtosecond laser light.[18] The upconversion spectra were consistent with previous work and the spectral bands assigned to Er^{III} radiative transitions. We characterized the power-dependent upconversion intensities after excitation with CW and femtosecond laser, and compared the experimental results with a light-matter interaction model containing 18 energy levels describing Nd^{III}, Yb^{III}, and Er^{III}. The simulations allowed characterization of population kinetics and power-dependence of the UCNP emission with CW and femtosecond excitation.

In the present work, we explore the concept of timescale integration using UCNP as a model system. We integrate optical trapping, stochastic dynamics and light-matter interactions experiments and simulations to evaluate the power dependence of single co-doped Yb^{III}:Er^{III} upconversion nanoparticles starting from their individual trajectories.

Simulations

First, we solve the overdamped Langevin equation of motion for a two-dimensional UCNP Brownian particle under the influence of a harmonic trapping force, as described previously [2,17,19]:

$$\frac{d\vec{r}}{dt} = -\frac{1}{\gamma}\vec{k}\cdot\vec{r} + \sqrt{2D}\xi(t)$$
$$\langle \xi(t)\xi(t') \rangle = 2k_B T\delta(t-t')$$

where γ is the friction coefficient, k is the trapping force constant, D is the diffusion coefficient, ξ is the white noise, k_B is Boltzmann's constant, and T is the temperature. Simulated conditions of temperature, particle size, medium viscosity, and laser beam profile/force constant were modelled after the experimental conditions described below. For the coupled stochastic-spectroscopic dynamics simulations, at each time step we determine the particle location and the incident light intensity at that location, assuming a two-dimensional Gaussian beam profile for the second, excitation laser, which an excitation source for the UCNPs studied in the present work.

The rate expressions describing light-matter interactions for the Yb^{III}:Er^{III} energy-level diagram shown in Figure 1 [20-22] are evaluated, with two levels describing Yb^{III} and levels for Er^{III} electronic states, where we model light absorption, non-radiative decay, energy transfer and radiative emission, as described in the Supporting Information. The initial ground-state lanthanide ion populations are parameterized after the experimental chemical composition of the UCNPs, and the remaining spectroscopic constants are as described previously.[18] For the coupled stochastic-spectroscopic dynamics simulations, from the particle position calculated using the Langevin equation, and from the associated intensity at that position (see previous paragraph), we solve the light-matter kinetic equations for the energy-level diagram shown in Figure 1. We have studied two different conditions for the time-step update: (i) resetting the populations to their initial ground-state populations at each time step; (ii) alternatively, we employ the steady-state populations calculated in each time step for the next time step during the coupled simulations. In both cases, the power law can be retrieved, although at different incident laser intensity levels (lower intensity in case ii).

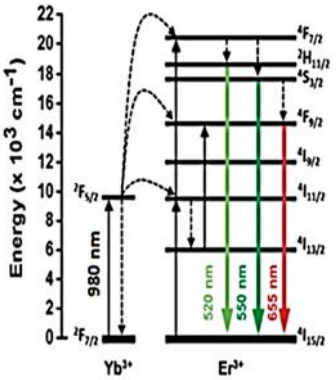

Figure 1. Energy-level diagram for the pair of Yb^{III}:Er^{III} ions studied in this work.

From the photophysics simulations, steady-state populations for each quantum state shown in Figure 1 are reached on a timescale shorter than the Brownian dynamics timestep. The plot of Er^{III} $^2H_{11/2}$ population as a function of input intensity is calculated "on the fly" as the Brownian

particle moves in the presence of an inhomogeneous light intensity distribution.[23] In this way, individual trajectories enable assessment of the power dependence of UCNP upconversion emission as a function of incident light intensity.

Experimental Section

Upconversion nanoparticle samples with the matrix β-$NaYF_4$:Er^{III}(2%),Yb^{III}(20%), were synthesized as described in references.[24,25] The samples were characterized by high-resolution scanning electron microscopy, powder X-ray diffraction, and down- and up-conversion luminescence. For the optical trapping and microscopy measurements, the samples were diluted in a series of solvents at an average concentration of 1.5 mg/mL to determine which would give a better dispersion of the nanoparticles. Prior to the measurements, the samples were taken to a tip sonicator to ensure particle dispersion and colloidal stability, which was checked by dynamic light scattering (DLS) particle size measurement. Upconversion microscopy and optical tweezers measurements were performed as described previously [26,27]. Briefly, a 975 nm laser beam is sent to a nonlinear microscope set up in a vertical, epifluorescence geometry. In the experiments, a single laser beam is used to excite and exert force on the UCNPs. Luminescence is collected and sent to a camera and spectrometer for images and spectral measurements, respectively. Quantitative analysis of particle position and emission intensities is performed with ImageJ.[28]

Results and Discussion

As shown in Figure 2, we have studied the coupled stochastic-spectroscopic dynamics of UCNPs under three dynamical conditions: (i) as the UCNP moves towards the trap (Figures 2A and 2D and Movie S1); (ii) optically trapped UCNP (Figures 2B and 2E and Movie S2); and (^{III}) UCNP undergoing Brownian motion in the absence of trapping (Figures 2C and 2F and Movie S3), that is, with trapping force constant set to zero in the simulations while still in the presence of spatially-varying low light intensities. For each condition shown in Figure 2, the results in the first column show calculated stochastic particle position trajectory overlaid on the trapping/excitation laser intensity profile, while the results in the second column show the results of power law characterization evaluated “on the fly” from the corresponding stochastic trajectories shown on the left. To aid visualization, the calculated stochastic trajectories are a few seconds in duration and thus consist of several thousand diffusive time steps. Running the simulations for larger number of time steps and longer simulation times gives the same overall conclusions discussed below, except that data oversampling at the equilibrium UCNP particle position is observed with increasing simulation time (Figures S1 and S2).

Figures 2A and 2D show the case where the particle moves closer to the trap center as it undergoes Brownian motion according to the Langevin equation. The stochastic trajectory shows that the UCNP particle samples incident light intensities ranging from very weak (distant from the trap center) to strongest (at the trap center). As the particle moves closer to the trap center, it experiences stronger light intensity. Conversely, at each particle location, the incident light drives the light-matter interactions according to the energy-level diagram shown in Figure 1, thus affecting the steady-state Er^{III} $^2H_{11/2}$ population and upconversion emission intensity.

After solving the light-matter interaction simulations for the Yb^{III}: Er^{III} UCNP system for a duration equal to one Brownian time step, the population in each quantum state reached steady-state. Then, the Brownian UCNP particle moves forward in time to a new position - and hence excitation intensity - according to the overdamped Langevin equation. As a result, the power law plot on the right (Figure 2D) gives the calculated nonlinear optical response of the Yb^{III}:Er^{III} co-doped UCNP over a large range of incident intensities. Specifically, from the resulting stochastic trajectory, we calculated the normalized UCNP emission intensity as a function of

light intensity, and the data is plotted in a log-log scale to show the power law more clearly. Figure 2D thus shows that upconversion is a two-photon process in this case, as expected from the given Yb^{III}:Er^{III} energy-level diagram in Figure 1 and the light-matter interaction equations (see Supporting Information) solved in the low-intensity regime. These general conclusions, discussed in connection with Figures 2A and 2D, show that it is possible to obtain the power law for the Brownian UCNP particle, and the same conclusions can be reached at for the trajectories of optically trapped and freely diffusing UCNPs as well (Figures 2B/2E and 2C/2F, respectively).

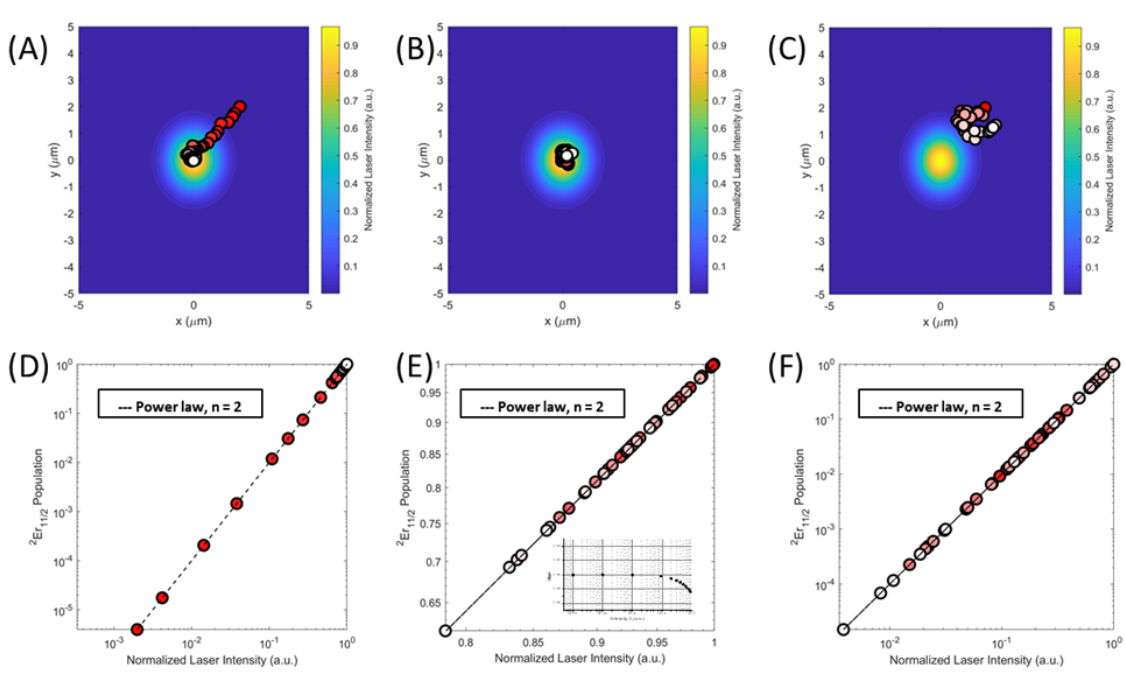

Figure 2. Spectroscopic-stochastic simulations. Top row: Simulated stochastic trajectory of a Brownian UCNP particle overlaid on a contour diagram of the laser/trapping beam intensity profile. The UCNP particle center position is colored with an interpolation from red to white as the stochastic trajectory moves forward in time. Bottom row: Population of Er $^2H_{11/2}$ level as a function of input intensity retrieved from the stochastic trajectory shown above, and a curve for a power law equal to two (dashed line). Here, the circle colors match the trajectory color scheme shown in the stochastic trajectories. Figures 2A/2D: UCNP particle moving towards the trap; Figures 2B/2E: optically trapped UCNP particle; Figures 2C/2F: freely diffusing UCNPs.

Figures 2B and 2E show that the power law behaviour can also be retrieved in the case of stochastic dynamics when the initial UCNP particle position is near the excitation beam centre position, that is, the UCNP is already optically trapped at the beginning of the simulation. The range of intensities sampled by the Brownian particle is smaller in this case when compared with Figures 2A and 2D. Nonetheless, the stochastic trajectory shown in Figure 2B can also be used for characterization of the UCNP nonlinear optical response. As shown in Figure 2E, the two-photon upconversion mechanism with a power law equal to two is observed for the range of intensities sampled in Figure 2B. Furthermore, the effect of initial input intensity is shown in the inset of Figure 2E. At low input intensities, a two-photon mechanism is observed. However, at higher intensities, the two-photon mechanism discussed above is replaced by power law behavior in which the “slope” decreases with increasing intensity, as discussed previously

[17,29]. Nonetheless, the resulting power law can be characterized with this approach as well (Figure S3).

Figures 2C and 2F show results of coupled spectroscopic-stochastic simulations in the presence of a Gaussian excitation profile yet without harmonic trapping potential, which is relevant for experiments involving weaker laser beam intensities or negligible trapping stiffness. As a result, the UCNP particle undergoes ordinary Brownian motion (i.e., free diffusion). Additionally, it also samples a range of incident light intensities at different locations, thereby allowing characterization of the UCNP power dependence as well (see Figure S4 for full results on the effect of force constant on the retrieved power law).

Table 1. Parameter space studied in the spectroscopic / stochastic simulations (see Supporting Information).

Parameter	Range
Particle size (nm)	100 – 1000
Initial particle position (μm)	0 – 6
Ion concentration	10^2 – 10^{20}
Ion weight fraction (%)	1 – 99
Elements	Yb, Er, Gd, Nd, Tm
Force constant (x 10^6 fN/nm)	0.01 – 1
UCNP photophysics simulation time (ms)	0.05 – 1
Nonlinear optical power law	1.5 – 5

We have performed additional numerical studies for a range of parameters describing the particle composition, morphology, and light intensity, as summarized in Table 1 (see Supporting Information, Figures S3-S6). The range of chemical systems considered also included Gd^{III}, Nd^{III}, and Tm^{III} with different energy-level diagrams in each case, thus leading to nonlinear optical responses up to fifth-order being characterized from individual stochastic trajectories (Figure S7). Finally, we also note that the power dependence of UCNP emission was characterized in a range of nanoparticle radii (Figure S8), which thus enables the study of homogeneous as well as ensemble UCNP responses. Overall, the simulation results show that "on the fly" evaluation of UCNP power dependence from individual stochastic trajectories can be applied for the parameter space shown in Table 1, and we thus expect it to be generally applicable for other types of UCNPs.

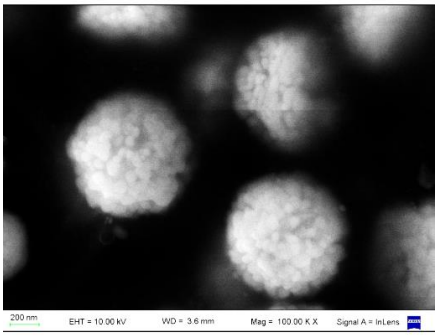

Figure 3. HRSEM image of Yb^{III}:Er^{III} co-doped UCNPs studied in the present work.

The UCNP samples were prepared as described in our previous work.[17,25] As shown in Figure 3, HRSEM revealed UCNP multifaceted particles with an average size of 600 □ 30 nm, consistent with our previous work. Prior to the optical microscopy measurements, UCNPs were dispersed in N,N-dimethylformamide solvent and characterized by dynamic light scattering. Furthermore, ensemble upconversion power dependence measurements for Yb^{III}:Er^{III} UCNPs are consistent with the energy diagram shown in Figure 1 and previous work [29].

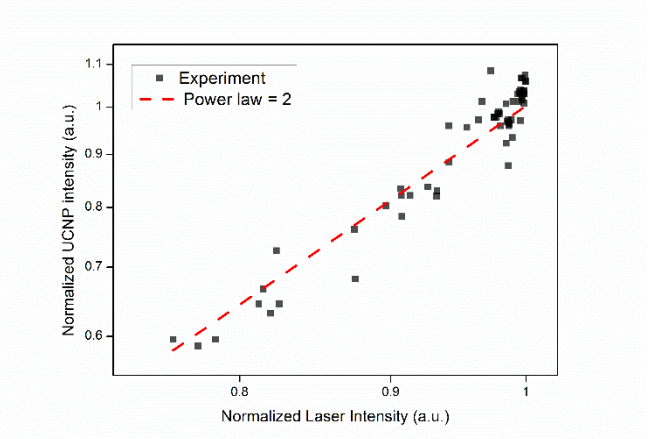

Figure 4. Single UCNP emission intensity as a function of normalized excitation intensity (black squares) and a curve for a power law equal to two.

The experimental setup used for characterizing UCNP motion and upconversion luminescence consisted of an optical trapping setup with NIR excitation coupled to an inverted optical microscope, as described previously.[17] Briefly, when the UCNPs are placed on the microscope, they interact with a 975 nm laser used for both optical trapping and upconversion luminescence. From recorded single UCNP trajectories, we quantify UCNP position and the emission intensity at each location, and thus the single-particle trajectories can be used to retrieve the UCNP power law for each experimental condition. Employing this approach for three different particles, Figure 4 shows the UCNP emission intensities as a function of incident intensity (black squares) together with a straight line corresponding to a power law equal to two. Thus, Figure 4 shows the power-dependence can be retrieved at the single UCNP level. Good agreement between experiments and simulations was obtained in the case where the simulations correspond to case (ii) (see Simulations section).

Several improvements in the strategy presented herein should be made to enable a better comparison between experimental and simulated results, and to extend the applicability of this approach. For example, complete parameterization of the energy-level shown in Figure 1 based on experimental results will require further spectroscopic studies of all the photophysical processes involved and lead to a better model for UCNPs with improved theoretical understanding of the photophysics.[30-46] For lanthanide-containing coordination complexes and clusters as well as smaller UCNPs,[47,48] the resulting faster diffusion will require new approaches, such as, for example, simulations incorporating ballistic dynamics combined with optical micro-spectroscopy experiments at higher frame rates. Furthermore, in such cases, the spectroscopic-stochastic dynamics may involve emitting quantum states in non-stationary populations, without clear timescale separation between photophysics and Brownian motion as shown here.

Conclusion

In conclusion, integrated optical trapping, stochastic dynamics and light-matter interactions experiments and simulations are used to evaluate the power dependence of single co-doped

Yb^{III}:Er^{III} upconversion nanoparticles starting from their individual trajectories. Overall, when compared with UCNP nonlinear optical response characterization in the far field, which requires varying the excitation pump power between measurements, in the combined spectroscopic-stochastic approach a single far-field input intensity is used. This strategy may be useful for single nanoparticle characterization of the nonlinear optical response, while the far-field approach is better for ensemble measurements.

Despite the relative simplicity of the model system considered herein, we hope that the present work contributes to the growing literature on theoretical, computational, and experimental studies aimed at integrating dynamical information occurring at different timescales, from events occurring at the level of fundamental ballistic and diffusive dynamics all the way up to real-time processes.

Acknowledgements

RAN acknowledged the support by CNPq INCT Catalysis (grant 444061/20185) and FAPESP (grants 2016/23430-9, 2019/27471-0).

[1] H. S. Chung, W. A. Eaton, Curr. Op. Struct. Biol. 2018, 48, 30-39.

[2] J. Gieseler, J. R. Gomez-Solano, A. Magazzù et al, Adv. Opt. Phot. 2021, 13,74-241.

[3] R. Arrigo, K. Badmus, F. Baletto et al, Faraday Disc. 2018, 208, 339-394.

[4] G. H. Oliveira, R. A. Nome, Curr. Op. Coll. & Int. Sci. 2019, 44, 208-219.

[5] Y. Goh, Y. H. Song, G. Lee, H. Bae, M. K. Mahata, K. T. Lee, Phys. Chem. Chem. Phys. 2018, 20, 11359-11368.

[6] M. K. Mahata, K. T. Lee, Nanoscale Adv. 2019, 1, 2372-2381.

[7] L. Trubb, A. C. Bruttomesso, S. V. Eliseeva, S. Petoud, J. A. Ramírez, B. C. Barja, Chem. Eur. J. 2020, 26, 12645-12653.

[8] E. Venturini Filho, P. C. de Sousa Filho, O. A. Serra, I. T. Weber, M. A. M. Lucena, P. P. Luz, J. Lumin. 2018, 202, 89-96.

[9] F. Auzel, Chem. Rev. 2014, 104, 139-173.

[10] D. Jing, P. Xi, B. Wang, L. Zhang, J. Enderlein, A. M. van Oijen, Nat. Meth. 2018, 15, 415-423.

[11] P. Haro-González, B. del Rosal, L. M. Maestro, E. M. Rodríguez, R. Naccache, J. A. Capobianco, K. Dholakia, J. G. Solé and D. Jaque, Nanoscale 2013, 5, 12192-12199.

[12] H. Dong, L.-D. Sun, C.-H. Yan, Chem. Soc. Rev. 2015, 44, 1608.

[13] M. Pollnau, D. R. Gamelin, S. R. Luthi, H.U. Gudel, M. P. Hehlen, Phys. Rev. B, 2000, 61, 3337-3346.

[14] F. T. Rabouw, P. T. Prins, P. Villanueva-Delgado, M. Castelijns, R. G. Geitenbeek, A. Meijerink, ACS Nano 2018, 12, 4812-4823.

[15] V. I. Sokolov, A. V. Zvyagin, S. M. Igumnov, S. I. Molchanova, M. M. Nazarov, A. V. Nechaev, A. G. Savelyev, A. A. Tyutyunov, E. V. Khaydukova, V. Ya. Panchenko, Opt. Spect. 2015, 118, 609-613.

[16] P. C. de Sousa Filho, J. Alain, G. Leménager, E. Larquet, J. Fick, O. A. Serra, T. Gacoinde, J. Phys. Chem. C 2019, 123, 2441-2450.

[17] R. A. Nome, C. Sorbello, M. Jobbagy, B. C. Barja, V. Sanches, J. S. Cruz, V. F. Aguiar, Meth. App. Fluor. 2017, 5, 014005.

[18] G. H. Oliveira, F. S. Ferreira, G. F. Ferbonink, M. P. Belançon, F. A. Sigoli, R. A. Nome, J. Lumin. 2021, 234, 117953.

[19] P. H. Jones, O. M. Maragò, G. Volpe "Optical Tweezers: Principles and Applications", Cambridge University Press (2015).

[20] M. Pollnau, P. J. Hardman, W.A. Clarkson et al Optic Commun. 1998, 147 203-211.

[21] B.-C. Hwang, S. Jiang, T. Luo, et al, J. Opt. Soc. Am. B 2000, 17 833.

[22] Y. Hu, S. Jiang, G. Sorbello et al J. Opt. Soc. Am. B 2001, 18 1928.

[23] N. Sule, S. A. Rice, S. K. Gray, N. F. Scherer, Opt. Expr. 2015, 23, 29978.

[24] X. Ye, J. E. Collins, Y. Kang, J. Chen, D. T. N. Chen, A. G. Yodh, C. B. Murray, Proc. Natl. Acad. Sci. 2010, 107, 22430-22435.

[25] C. Sorbello, P. Gross, C.A. Strassert, M. Jobbágy B. C. Barja ChemPhysChem, 2017, 18, 1407-1414.

[26] G. H. Oliveira, M. T. Galante, T. T. Martins, et al, Solar Energy 2019, 190, 239-245.

[27] J. C. Franco, G. Gonçalves, M. S. Souza, et al, Opt. Exp. 2013, 21, 30874-30885.

[28] https://imagej.nih.gov/ij/

[29] F. A. Sigoli, R. R. Gonçalves, Y. Messaddeq, S. J. L. Ribeiro, J. Non-Cryst. Solids, 2006, 352, 3463-3468.

[30] G. Liu, Chem. Soc. Rev., 2015, 44 1635-1652.

[31] L. Tu, X. Liu, F. Wu, H. Zhang, Chem. Soc. Rev., 2015, 44 1331.

[32] T. Jung, H. L. Jo, S. H. Nam, B. Yoo, Y. Cho, J. Kim, H. Min, Kim, T. Hyeon, Y.D. Suh, H. Lee, K. T. Lee, Phys. Chem. Chem. Phys., 2015, 17 13201.

[33] I. M. S. Diogenis, E. M. Rodrigues, I. O. Mazali, F. A. Sigoli, J. Lumin, 2021, 232, 117848

[34] K. Shin, T. Jung, E. Lee, G. Lee, Y. Goh, J. Heo, M. Jung, E-J. Jo, H. Lee, M.-G. Kim, K. T. Lee, Phys. Chem. Chem. Phys. 2017, 19, 9739-9744

[35] E. Lee, M. Jung, Y. Han, G. Lee, K. Shin, H. Lee, K.T. Lee, J. Phys. Chem. C, 2017, 121, 38, 21073–21079

[36] A. Baride, P. Stanley May Jr, M.T. Berry, J. Phys. Chem. C, 2020, 124, 2193−2201

[37] T.A. Laurence, Y. Liu, M. Zhang, M.J. Owen, J. Han, L. Sun, C. Yan, G-y. Liu, J. Phys. Chem. C, 2018, 122, 23780−23789.

[38] J. Liu, T. Fu, C. Shi J. Phys. Chem. C, 2019, 123, 9506−9515.

[39] M.D. Wisser, S. Fischer, C. Siefe, A.P. Alivisatos, A. Salleo, J.A. Dionne, Nano Lett., 2018, 18, 2689−2695

[40] C. Ma, X. Xu, F. Wang, Z. Zhou, D. Liu, J. Zhao, M. Guan, C.I. Lang, D. Jin Nano Lett., 2017, 17, 2858−2864

[41] M.Y. Hossan, A. Hor, Q. Luu, S. J. Smith, P.S. May, M.T. Berry J. Phys. Chem. C, 2017, 121, 16592−16606

[42] M.T. Berry, P.S. May, J. Phys. Chem. A, 2015, 119, 9805−9811

[43] J.M. Bujjamer, M.C. Marchi, B.C. Barja, H.E. Grecco, En. Rep, 2020, 6 63–69

[44] R.T. Moura Jr., A.N.C. Neto, R.L. Longo, O.L. Malta, J. Lumin. 2021, 170, 420-430.

[45] R.E. Joseph, C. Jiménez, D. Hudry, G. Gao, D. Busko, D. Biner, A. Turshatov, K. Krämer, B.S. Richards, I.A. Howard, J. Phys. Chem. A, 2019, 123, 6799-6811.

[46] B. Chen, F. Wang, TRECHM, 2020, 2, 427-439.

[47] S.H. Nam, Y.M. Bae, Y.I. Park, J.H. Kim, H.M. Kin, J.S. Choi, K.T. Lee, T. Hyeon, Y.D. Suh, Angew. Chem., 2011, 50(27) 6093-6097.

[48] D.A. Gálico, J.S. Ovens, F.A. Sigoli, M. Murugesu, ACS Nano 2021, 15, 5580-5585.

SUPPORTING INFORMATION

"On the fly" characterization of Yb^{III}:Er^{III} co-doped upconversion nanoparticle nonlinear optical response from single-particle trajectories

Isabela N. Cavalcante, M. Claudia Marchi, Fernando A. Sigoli, Paulo C. de Sousa Filho, Beatriz C. Barja,* and René A. Nome*

Corresponding authors:

* nome@unicamp.br

* barja@qi.fcen.uba.ar

RATE EQUATION FOR THE ENERGY DIAGRAM SHOWN IN FIGURE 1

$$\frac{d\,n_{Yb^{III}\,^2F_{5/2}}}{dt} = -W_{DYb^{III}\,^2F_{5/2}\_AEr^{III}\,^4I_{11/2}} n_{Yb^{III}\,^2F_{5/2}} n_{Er^{III}\,^4I_{15/2}}$$
$$-W_{DYb^{III}\,^2F_{5/2}\_AEr^{III}\,^4F_{9/2}} n_{Yb^{III}\,^2F_{5/2}} n_{Er^{III}\,^4I_{13/2}} - W_{DYb^{III}\,^2F_{5/2}\_AEr^{III}\,^4F_{7/2}} n_{Yb^{III}\,^2F_{5/2}} n_{Er^{III}\,^4I_{11/2}}$$
$$-W_{DYb^{III}\,^2F_{5/2}\_AEr^{III}\,^2H_{9/2}} n_{Yb^{III}\,^2F_{5/2}} n_{Er^{III}\,^4F_{9/2}}$$

$$\frac{d\,n_{Yb^{III}\,^2F_{7/2}}}{dt} = W_{DYb^{III}\,^2F_{5/2}\_AEr^{III}\,^4I_{11/2}} n_{Yb^{III}\,^2F_{5/2}} n_{Er^{III}\,^4I_{15/2}}$$
$$+W_{DYb^{III}\,^2F_{5/2}\_AEr^{III}\,^4F_{9/2}} n_{Yb^{III}\,^2F_{5/2}} n_{Er^{III}\,^4I_{13/2}} + W_{DYb^{III}\,^2F_{5/2}\_AEr^{III}\,^4F_{7/2}} n_{Yb^{III}\,^2F_{5/2}} n_{Er^{III}\,^4I_{11/2}}$$
$$+W_{DYb^{III}\,^2F_{5/2}\_AEr^{III}\,^2H_{9/2}} n_{Yb^{III}\,^2F_{5/2}} n_{Er^{III}\,^4F_{9/2}}$$

$$\frac{d\,n_{Er^{III}\,^2H_{9/2}}}{dt} = W_{DYb^{III}\,^2F_{5/2}\_AEr^{III}\,^2H_{9/2}} n_{Yb^{III}\,^2F_{5/2}} n_{Er^{III}\,^4F_{9/2}} - \frac{n_{Er^{III}\,^2H_{9/2}}}{\tau_{r,Er^{III}\,^2H_{9/2}\rightarrow Er^{III}\,^4I_{15/2}}}$$

$$\frac{d\,n_{Er^{III}\,^4F_{7/2}}}{dt} = W_{DYb^{III}\,^2F_{5/2}\_AEr^{III}\,^4F_{7/2}} n_{Yb^{III}\,^2F_{5/2}} n_{Er^{III}\,^4I_{11/2}} - n\frac{Er^{III}\,^4F_{7/2}}{\tau_{nr,Er^{III}\,^4F_{7/2}\rightarrow Er^{III}\,^2H_{11/2}}}$$

$$\frac{d\,n_{Er^{III}\,^2H_{11/2}}}{dt} = \frac{n_{Er^{III}\,^4F_{7/2}}}{\tau_{nr,Er^{III}\,^4F_{7/2}\rightarrow Er^{III}\,^2H_{11/2}}} - \frac{n_{Er^{III}\,^2H_{11/2}}}{\tau_{nr,Er^{III}\,^2H_{11/2}\rightarrow Er^{III}\,^4S_{3/2}}} - \frac{n_{Er^{III}\,^2H_{11/2}}}{\tau_{r,Er^{III}\,^2H_{11/2}\rightarrow Er^{III}\,^4I_{15/2}}}$$

$$\frac{d\,n_{Er^{III}\,^4S_{3/2}}}{dt} = \frac{n_{Er^{III}\,^4S_{3/2}}}{\tau_{nr,Er^{III}\,^2H_{11/2}\rightarrow Er^{III}\,^4S_{3/2}}} - \frac{n_{Er^{III}\,^4S_{3/2}}}{\tau_{r,Er^{III}\,^4S_{3/2}\rightarrow Er^{III}\,^4I_{15/2}}} - \frac{n_{Er^{III}\,^4S_{3/2}}}{\tau_{nr,Er^{III}\,^4S_{3/2}\rightarrow Er^{III}\,^4F_{9/2}}}$$

$$\frac{d\,n_{Er^{III}\,^4F_{9/2}}}{dt} = \frac{n_{Er^{III}\,^4S_{3/2}}}{\tau_{nr,Er^{III}\,^4S_{3/2}\rightarrow Er^{III}\,^4F_{9/2}}} - \frac{n_{Er^{III}\,^4F_{9/2}}}{\tau_{r,Er^{III}\,^4F_{9/2}\rightarrow Er^{III}\,^4I_{15/2}}}$$
$$+W_{DYb^{III}\,^2F_{5/2}AEr^{III}\,^4F_{9/2}} n_{Yb^{III}\,^2F_{5/2}} n_{Er^{III}\,^4I_{13/2}} - W_{DYb^{III}\,^2F_{5/2}\_AEr^{III}\,^2H_{9/2}} n_{Yb^{III}\,^2F_{5/2}} n_{Er^{III}\,^4F_{9/2}}$$

$$\frac{d\,n_{Er^{III}\,^4I_{11/2}}}{dt} = -\frac{n_{Er^{III}\,^4I_{11/2}}}{\tau_{nr,Er^{III}\,^4I_{11/2}\rightarrow Er^{III}\,^4I_{13/2}}}$$
$$-W_{DYb^{III}\,^2F_{5/2}AEr^{III}\,^4F_{7/2}} n_{Yb^{III}\,^2F_{5/2}} n_{Er^{III}\,^4I_{11/2}} + W_{DYb^{III}\,^2F_{5/2}AEr^{III}\,^4I_{11/2}} n_{Yb^{III}\,^2F_{5/2}} n_{Er^{III}\,^4I_{15/2}}$$

SIMULATION RESULTS FOR THE SPECTROSCOPIC-STOCHASTIC CHARACTERIZATION OF UPCONVERSION

MOVIES S1-S3: stochastic dynamics trajectories and associated on-the-fly upconversion characterization (see attached)

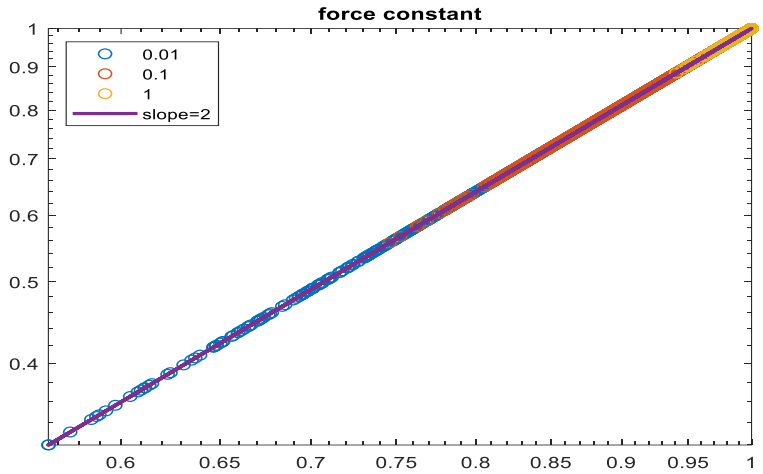

Figure S1: $Er^2H_{11/2}$ population as a function of normalized laser intensity for various values of the force constant with Brownian timestep of 50 μs.

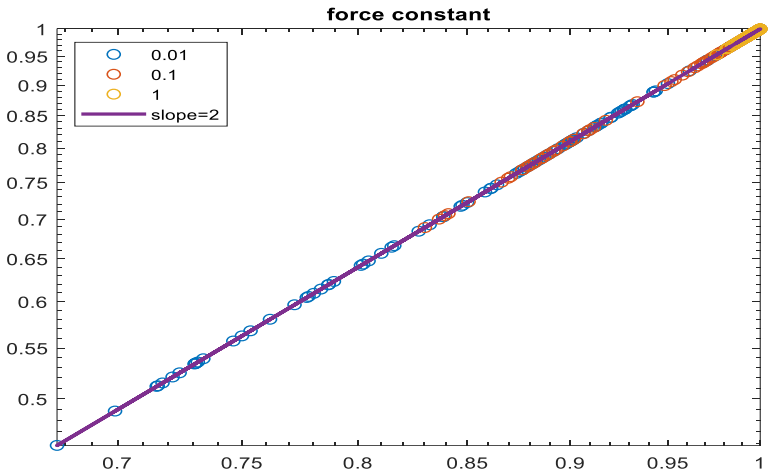

Figure S2: $Er^2H_{11/2}$ population as a function of normalized laser intensity for various values of the force constant with Brownian timestep of 1 ms.

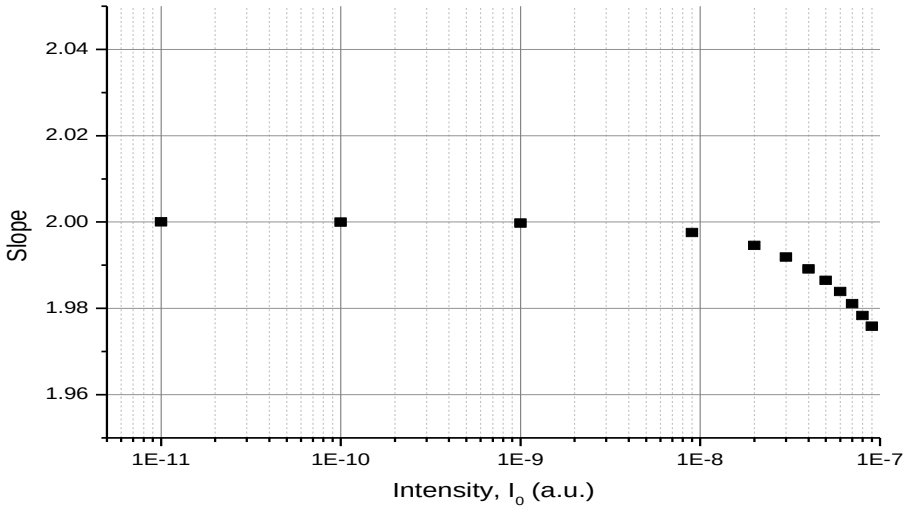

Figure S3: Power law slope as a function of incident intensity

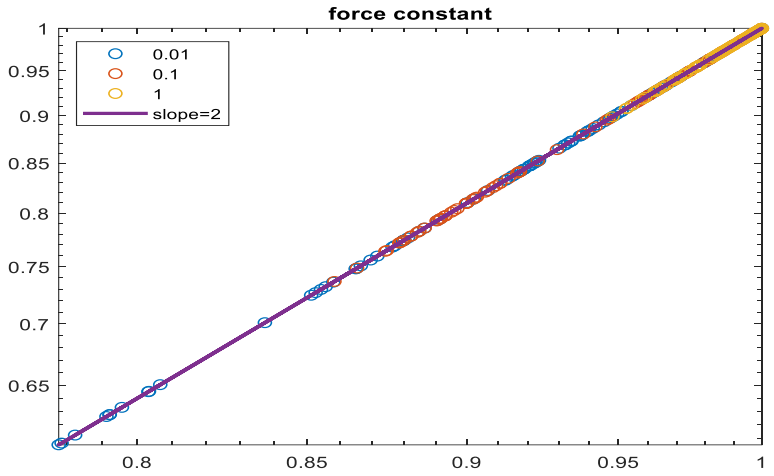

Figure S4: $Er^2H_{11/2}$ population as a function of normalized laser intensity for various values of the force constant.

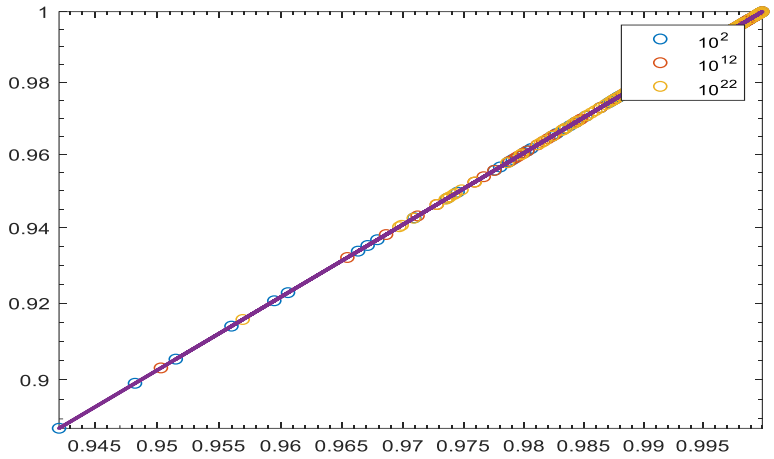

Figure S5: $Er^2H_{11/2}$ population as a function of normalized laser intensity for various values of the lanthanide ion concentration.

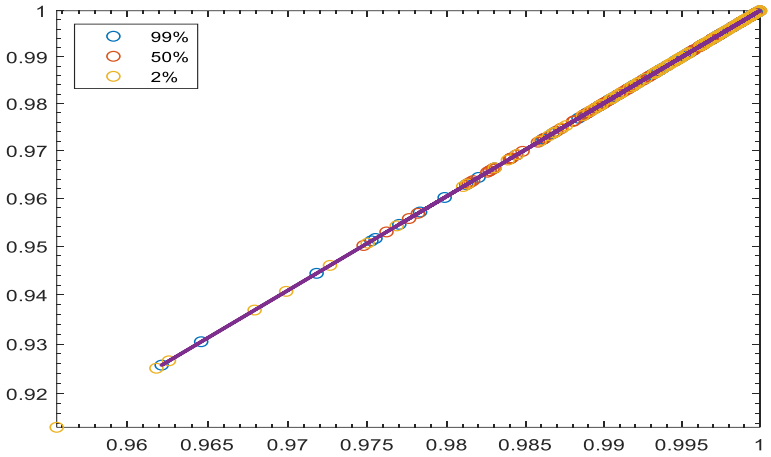

Figure S6: $Er^2H_{11/2}$ population as a function of normalized laser intensity for various values of Yb^{III}:Er^{III} fraction.

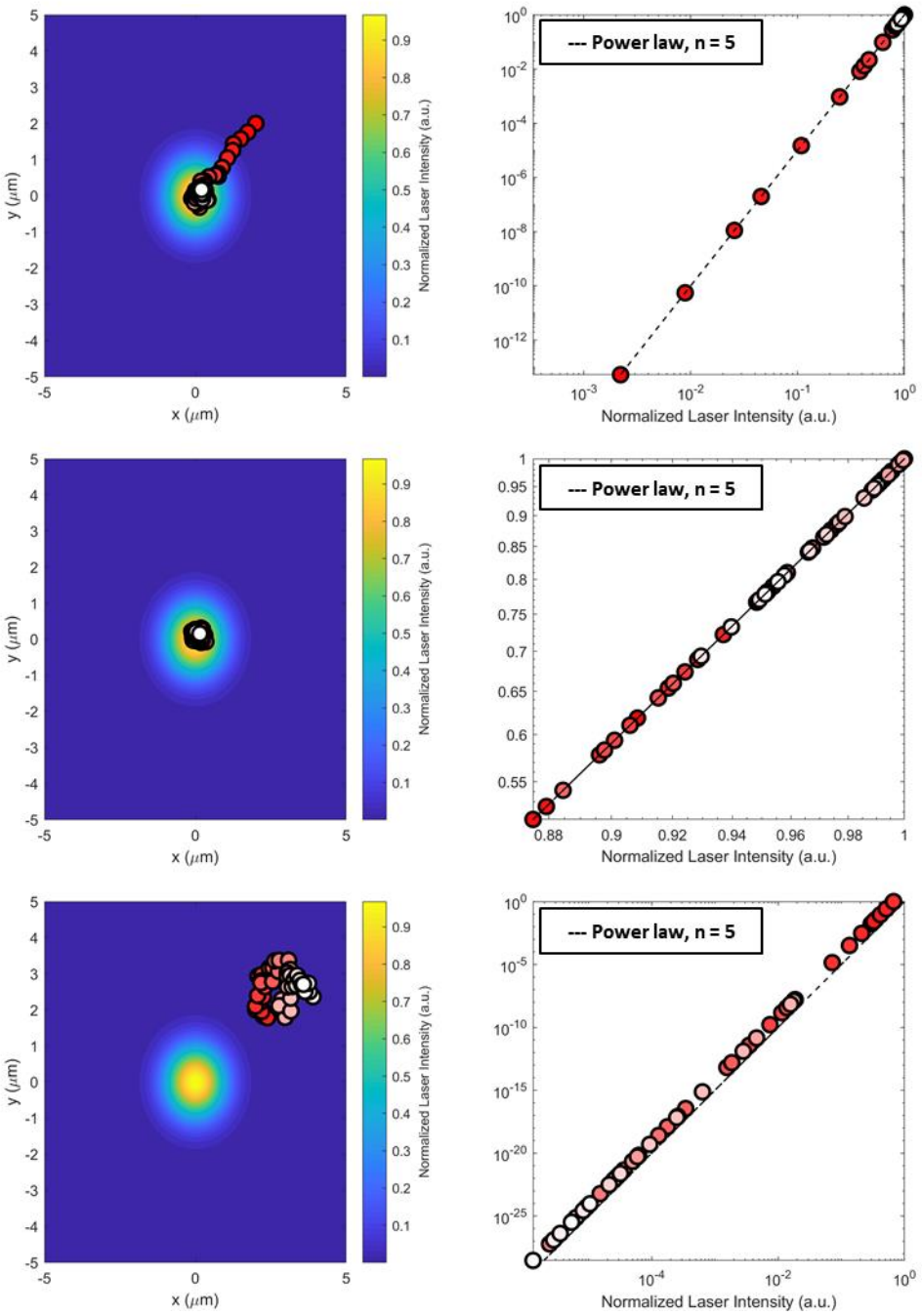

Figure S7. Spectroscopic-stochastic simulations for system with 5th order nonlinear response.

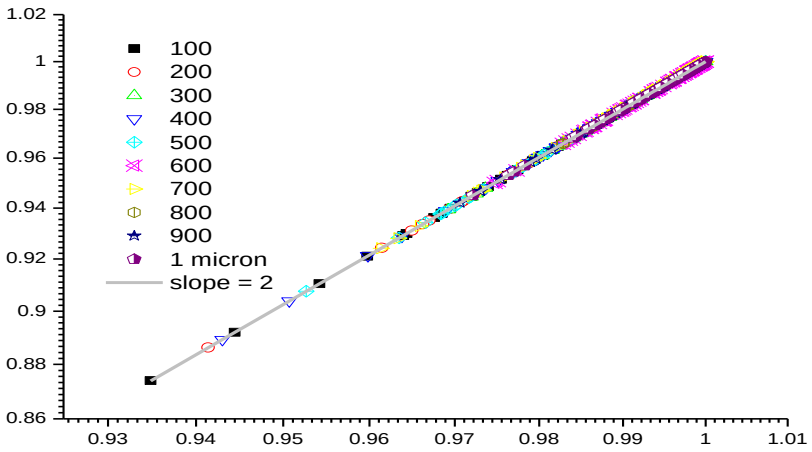

Figure S8: $Er^2H_{11/2}$ population as a function of normalized laser intensity for various nanoparticle dimensions (in nm).